Electrical activity at grain boundaries of $Cu(In,Ga)Se_2$ thin films

D. Fuertes Marrón,* S. Sadewasser,† A. Meeder,‡ Th. Glatzel, and M. Ch. Lux-Steiner
Department of Solar Energy, Hahn-Meitner Institut Berlin, Glienicker Strasse 100, D-14109 Berlin, Germany
(Received 1 July 2004; revised manuscript received 8 October 2004; published 6 January 2005)

There is a renewed interest in the electrical activity at grain boundaries in relation to the outstanding performance of thin film solar cells based on $Cu(In,Ga)Se_2$. We observed electrical activity at grain boundaries in $CuGaSe_2$ thin films by locally resolved work function measurements, using Kelvin probe force microscopy in ultrahigh vacuum on *in situ* prepared surfaces. By means of their electrical activity under illumination, we identify different types of grain boundaries, presumably associated with different crystallite orientations. A comprehensive discussion of the applicability of different models is presented.

DOI: 10.1103/PhysRevB.71.033306 PACS number(s): 73.50.Pz, 73.30.+y, 73.40.Lq

In comparison to grain boundaries (GBs) in Si,[1] those in chalcopyrite semiconductors are by far not as well studied nor understood. Only very recently have some experimental[2–4] and theoretical studies[5] been conducted, motivated by the remarkably high solar energy conversion efficiencies of polycrystalline absorbers compared to those obtained so far from single-crystalline ones. However, this comparison appears slightly biased: crystalline chalcopyrite solar cells have not received nearly as much effort in the optimization as high efficiency thin film devices (see, for example, the elaborate band gap engineering exercises in NREL's three stage process[6]). Reaching efficiency figures close to 20% from any type of polycrystalline absorber (including as well silicon or CdTe) necessarily requires a favorable behavior of the GBs. Experimental studies have demonstrated electrical effects at *p*-type chalcopyrite GBs, both indirectly by Hall and conductivity measurements[2] and directly using Kelvin probe force microscopy (KPFM);[4,7] results were explained according to a GB model developed by Seto for Si, which assumes a depletion layer in the near-GB region induced by some charge storage at interface states.[8] A typical band diagram for this "electronic" GB model for a chalcopyrite absorber has been reported, e.g., by Schuler *et al.* for $CuGaSe_2$.[2] It bends downwards some 100 meV, representing an electrostatic barrier for the transport of holes (typically majority carriers) and a sink for electrons (minority ones), as sketched in Fig. 1(a). The depletion region on either side of the GB plane results from positively charged interface states. This band bending has been observed directly by Sadewasser *et al.* by laterally resolved surface potential measurements using KPFM (Ref. 4) and recently confirmed by Jiang *et al.*[7] However, both studies used samples exposed to air, thus possible contamination affecting the GB electronics could not be excluded. The minor detrimental role attributed to GBs in polycrystalline films is accounted for within the frame of the "electronic" GB model by a certain reduction of the band bending at the GBs gained under illumination (i.e., under solar cell operating conditions), as a fraction of minority carriers are trapped at interface states, reducing the net stored charge and thus the associated electric field and depletion region.

In contrast to the "electronic" GB model, a recent theoretical study using first-principles modeling of GBs for selected grain orientations in $CuInSe_2$ proposed the appearance of an energetic barrier for holes arriving from the inner part of the grains without the presence of interface charge at GBs.[5] A reduced *p-d* hybridization between group-I-cation and chalcogen-anion states, due to Cu-vacancy surface reconstruction, was proposed to lead to an overall downward shift of the valence band maximum in the near-GB region, as schematically shown in Fig. 1(b). This model can indeed account for the experimental observations based on electronic transport measurements mentioned above. Furthermore, the absence of available free holes at GBs prevents electron recombination, minimizing the detrimental effects for electronic applications as a result of minority carrier loss. This "structural" GB model explicitly excludes built-in potentials (i.e., stored charge) at GBs. This is understood as the result of a self-compensation of electronic point defects by their arrangement into neutral pairs of the type $2V_{Cu}^{-}+In_{Cu}^{2+}$, despite the fact that some gettering activity of GBs (for different types of impurities and in particular for Na) is acknowledged in the model.

In *p*-type chalcopyrites (as used for solar cell absorbers), both GB models, the "electronic" and the "structural" one, lead to similar predictions for the behavior of majority carrier transport (i.e., in the electronics involved at energies below the Fermi level); however, they should be discernible on the basis of minority carrier effects at GBs, for example by measurement of the local electronic properties observed with a characterization tool allowing high lateral resolution in the nanometer range.

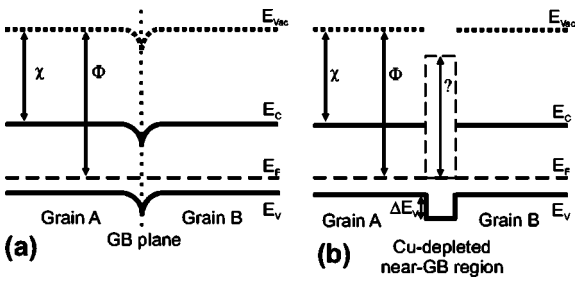

FIG. 1. Schematic band diagram at a grain boundary. (a) "Electronic" GB model explaining the electrical effects at GBs as a result of band bending induced by stored charge (Ref. 2) and (b) "structural" GB model, proposing a barrier for holes as a result of the GB stoichiometry (Ref. 5).

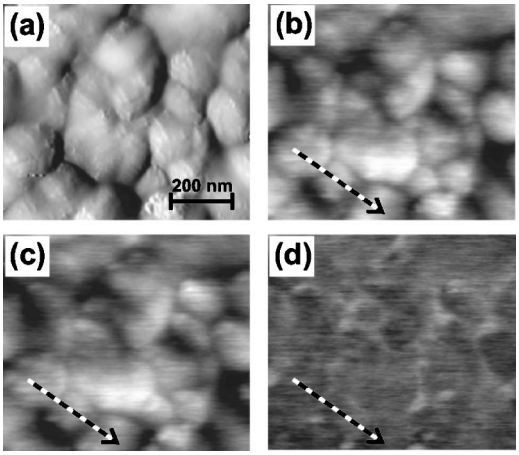

FIG. 2. KPFM measurement on the UHV-clean rear side of a $CuGaSe_2$ absorber film. (a) Topography (height range=92 nm), (b) work function in dark (4.79–4.94 eV), (c) work function under illumination (4.88–5.01 eV), and (d) SPV image (41–140 mV). Different GB types are distinguished by the presence or absence of SPV. The line represents the position of the line scan in Fig. 3.

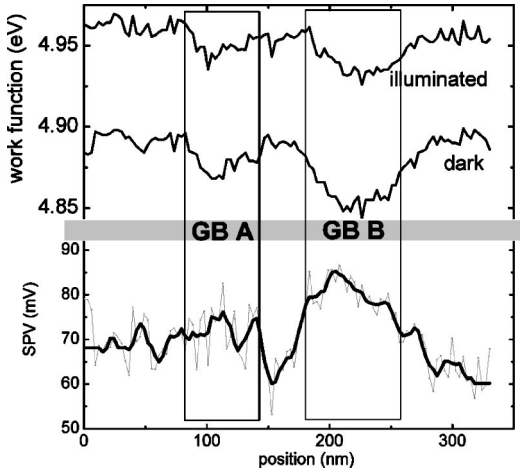

FIG. 3. Line scan along the line in Fig. 2. Upper panel: A drop in the work function (in darkness and under illumination) at the position of the GBs is observed. GBs *A* and *B* are of different types as indicated by their different SPV characteristic (lower panel); the line is a smoothed curve of the data (gray line).

In this Brief Report we present laterally resolved work function (Φ) measurements carried out by KPFM in ultrahigh vacuum (UHV). A UHV-clean rear surface of a chalcopyrite compound ($CuGaSe_2$—hereafter CGSe) is investigated, revealing distinct electrical activity at GBs. The results provide evidence for the presence of different types of GBs in the films, as distinguished by illumination effects. A comprehensive discussion of the applicability of the models described above is given.

Polycrystalline thin-film samples were grown in a two-stage process by chemical vapor transport onto Mo-coated soda-lime glass with slightly Ga-rich final composition as required for solar cell device processing ($\eta > 7\%$), and were peeled-off in UHV following a technique reported in detail elsewhere.[9,10] This sample preparation prevents postgrowth air exposure and surface contamination which may affect the extremely surface-sensitive contact potential measurements.[11] The cleanness of the procedure, i.e., the absence of substrate remnants after lifting the sample off, has been positively tested by means of *in situ* XPS measurements, revealing no traces of Mo on the CGSe rear surface.[10,12] Nonetheless, traces of oxygen and carbon have been found, which are attributed to air contamination of the Mo-surface prior to sample processing. KPFM measurements were performed using a modified Omicron UHV-AFM/STM ($p=10^{-10}$ mbar) capable of simultaneously measuring topography and contact potential between tip and sample.[13] PtIr-coated Si cantilevers were calibrated on a highly oriented pyrolytic graphite sample before and after each measurement, in order to obtain absolute work function values and to prove the stability of the tip.

The topography image of the CGSe rear surface [Fig. 2(a)] shows a granular texture, corresponding to the base of columnar grains (~ 3 μm long) with lateral dimensions between 50–400 nm; in contrast, typical grain widths at the film top surface lie in the micrometer range. GBs can be identified in the work function mapped in the dark in Fig. 2(b) by direct inspection and comparison to the topographical image, showing lower work function values than the crystallite surfaces. This effect is clearly seen along a representative line-scan shown in Fig. 3. Three adjacent grains build up GBs A and B. The work function lowering associated with the GBs is different in magnitude by a factor of approximately 2. Due to the flat topography of the absorber's rear surface (height range $\sim$90 nm), any possible influence of surface roughness on the work function measurement can be largely excluded.

It should be noted that this work function reduction at GBs is, in principle, not sufficient to exclude the applicability of the "structural" model: the results can still be interpreted in the frame of both "electronic" and "structural" GB models. In the first case the presence of positively charged interface states results in a downwards band bending at the GB [see Fig. 1(a)]. In the latter case, the electronic structure of the Cu-poor near-GB region above the Fermi level has to be considered, in particular regarding possible deviations from the inner grain electron affinity values. Persson and Zunger calculated the electron wave function for an energy corresponding to the conduction band minimum (CBM) of the grain interior, which appears nonvanishing and continuous through the near-GB region.[5] This finding is, however, not sufficient for assuming a flat conduction band at the GB. In fact, a CBM offset has been predicted by Zhang *et al.*[14] for the interface between 1:1:2/1:3:5 compounds (together with the postulated valence band offset found in Ref. 5), the latter compound being the result of the arrangement of those defect pairs contemplated in Ref. 5 leading to the Cu-poor-GB region.[15]

For an explanation of the observed work function reduction within the "structural" GB model, it is mandatory to call for the presence of an interface dipole at the transition from the grain interior to the GB phase, resulting in a step in the local vacuum level [as schematically indicated in Fig. 1(b)]. The possible presence of interface dipoles at such interfaces

is necessarily rather speculative; it is nevertheless interesting to contemplate possible scenarios in which dipoles may play a role in the present problem. The polar nature of free {112} anion- or cation-terminated facets (those selected in Ref. 5) makes them in principle highly instable in comparison to nonpolar facets, due to the corresponding high surface energy contribution arising from the surface dipole. It is well known, however, that {112} faceting occurs naturally on nonpolar-oriented films grown by epitaxy.[16] This energy instability of polar surfaces is compensated by means of defect and defect pair rearrangement of the type $2V_{Cu}^{-}+In_{Cu}^{2+}$, leading to a Cu depletion in the near surface region, which effectively reduces the dipole contribution at metal-terminated planes.[17,18] One would thus expect that the proposed mechanism responsible for GB formation led to a reduced interface dipole. Nevertheless, the polar character of metal-terminated planes can be enhanced by metal relocation, for instance by means of Na in the form of Na_{Cu}, a possibility which is explicitly considered in the "structural" model. Na would increase the polar character of the layer while maintaining the valence band offset expected from Cu depletion, due to lack of *d* levels. We thus cannot exclude the presence of dipoles for the discussion of the GBs, and consequently cannot exclude the "structural" GB model from the interpretation of the observed work function reduction at GBs in measurements conducted in the dark.

In the following we will present additional results providing more evidence regarding the distinction between the applicability of the two GB models. We base our study on the electronics at energies above the Fermi level, i.e., on the changes observed in the electrical activity at GBs induced by excess electrons, acting as minority carriers. If GBs were governed by "structural" (i.e., band offsets) rather than "electronic" (built-in potential) factors as described by the models, the impact of the excess minority carriers should only be minor. Illuminating the sample with super-band-gap light (laser diode, $\lambda = 675$ nm) results in an overall increase of the work function [Fig. 2(c)] which saturates at high intensities (~ 60 mW/cm^2), an effect attributed to a reduction of the surface band bending in the scanned (sample-vacuum) surface plane. In the ideal case high-intensity illumination should lead to flat band conditions in the scanning plane (for a critical discussion see Ref. 19). Even if flat band conditions are not achieved, the presence of surface photovoltage ($SPV = \Phi^{ill} - \Phi^{dark}$) implies (a) no pinning of the Fermi level (e.g., due to surface contaminants or a high density of surface states) takes place at the scanning plane and (b) the extension of the depletion region toward the inner part of the sample can be modulated by illumination. If the SPV at sufficiently high light intensities were the only effect recorded, we should expect a general shift of the work function at all scanned positions. In Fig. 2(d) a SPV image of the scanned area is presented, obtained by subtracting Fig. 2(b) (measured in darkness) from Fig. 2(c) (under illumination), which shows the presence of at least two distinct GB types, one showing a larger SPV than the grains (bright areas) and others which do not show up. A representative line scan in Fig. 3 shows a significant reduction of the work function drop recorded at GB *B* under illumination, together with the overall increase in work function attributed to SPV on the scanned surface plane; this shows up as a characteristic peak in the SPV line (bottom). At the same time, GB *A* shows almost no change under illumination. This leads us to conclude the existence of different types of GBs, presumably associated with particular crystallite orientations. This connection between crystallite orientation and GB electrical activity can explain the influence of film texturing on the performance of high efficiency solar cells, in addition to a favorable band alignment between absorber and buffer layers, a point which has not yet received sufficient attention (preliminary studies have been conducted recently[20]) and which may in our opinion be of fundamental importance for further device optimization.

The reduction of the potential barrier at GBs associated with illumination cannot be accounted for within the frame of the "structural" GB model under the exclusive premise of an interface dipole. The decrease of the work function fits, however, into the "electronic" GB model: a reduction of the potential barrier sketched in Fig. 1(a) is due to photogenerated minority carriers (electrons) being trapped at ionized donorlike electronic states at the GB. The mechanism of light-induced GB passivation within the "electronic" GB model does not seem to apply equally to all types of GBs. For example, the behavior of GBs of type *A*, which shows almost no change under illumination, might well be explained to a large extent by the "structural" GB model. On the other hand, the illumination-induced change in the GB of type *B* does require the "electronic" GB model. A semiquantitative analysis of GB properties within the "electronic" model can be performed according to the model developed by Seto for the case of moderate doping concentration of the crystallites.[4,8] The net doping concentration of the crystallites forming GB *B* is found to be $P_{net} = 1.8 \times 10^{16}$ cm^{-3}. The density of charged states located at boundary *B* can be estimated to $P_{gb} = 1.9 \times 10^{11}$ cm^{-2}; this is well below the estimated threshold leading to Fermi level pinning at the interface, $\sim 10^{13}$ cm^{-2} as reported by Rau *et al.*,[21] in clear agreement with the observed SPV effect. It should also be mentioned at this point that the overall film composition may also play a role in the GB issue. Specifically, Schuler's samples used for Hall measurements and explained within the frame of the "electronic" model were prepared under Cu-rich conditions.[2] As Cu depletion is generally related to Cu-poor overall compositions, it cannot be excluded that the proposed mechanism of GB formation in the "structural" model does not apply equally well to samples grown under Cu excess. In other words, the applicability of the "structural" and the "electronic" GB models for interpreting results may depend on the type of samples considered (including as well high- and/or low-band-gap chalcopyrites).

In summary, the results presented show the presence of GBs with distinct electrical activity in polycrystalline chalcopyrite thin films. The "electronic" GB model does represent an important contribution to the GB electronics. It is concluded that a single shift of the valence band at GBs resulting from a reduced *p-d* hybridization due to Cu depletion, as proposed in the "structural" GB model,[5] is not the only mechanism involved in the electronics of GBs. This is clearly indicated by the illumination-induced electronic activity, which is necessarily linked with deviations from crys-

tallite bulk electronic properties between the Fermi and local vacuum levels. However, we cannot exclude a contribution of the "structural" GB model. In this respect, Fig. 2(d) is representative of a scenario in which different types of GBs must be taken into account in order to fully understand the film electronics. A theoretical prediction of electron affinity values associated with Cu-poor compositions of chalcopyrite compounds and the possible presence of dipoles would certainly shed more light on the intriguing issue of the structural and electronic properties of GBs.

The authors are grateful to R. Klenk for helpful discussion and acknowledge financial support from the German Ministry for Research and Education (Contract No. 01SF0023).

*Electronic address: fuertes-marron@hmi.de
†Present address: Centro Nacional de Microelectrónica IMB-CSIC, Campus UAB, 08193 Barcelona, Spain.
‡Present address: Sulfurcell Solartechnik GmbH, Barbara McClintock Str. 11, 12489 Berlin, Germany.

[1] L. K. Fionova and A. V. Artemyev, *Grain Boundaries in Metals and Semiconductors* (Les Editions de Physique, Les Ulis Cedex, 1993), and references therein.
[2] S. Schuler, S. Nishiwaki, J. Beckmann, N. Rega, S. Brehme, S. Siebentritt, and M. Ch. Lux-Steiner, in Proceedings of the 29th IEEE Photovoltaic Specialist Conference (IEEE, Piscataway, NJ, 2002), p. 504.
[3] S. Siebentritt and S. Schuler, J. Phys. Chem. Solids **64**, 1621 (2003).
[4] S. Sadewasser, Th. Glatzel, S. Schuler, S. Nishiwaki, R. Kaigawa, and M. Ch. Lux-Steiner, Thin Solid Films **431–432**, 257 (2003).
[5] C. Persson and A. Zunger, Phys. Rev. Lett. **91**, 266401 (2003).
[6] K. Ramanathan, M. A. Contreras, C. L. Perkins, S. Asher, F. S. Hasoon, J. Keane, D. Young, M. Romero, W. Metzger, R. Noufi *et al.*, Prog. Photovoltaics **11**, 225 (2003).
[7] C.-S. Jiang, R. Noufi, J. A. Abu Shama, K. Ramanathan, H. R. Moutinho, J. Pankow, and M. M. Al-Jassim, Appl. Phys. Lett. **84**, 3477 (2004).
[8] J. Y. W. Seto, J. Appl. Phys. **46**, 5247 (1975).
[9] D. Fuertes Marrón, A. Meeder, R. Würz, S. M. Babu, M. Rusu, Th. Schedel-Niedrig, and M. Ch. Lux-Steiner, in Proceedings of the International Conference PV in Europe, From Technology to Energy Solutions (WIP, Munich, and ETA, Florence, 2002), p. 421.
[10] D. Fuertes Marrón, A. Meeder, R. Würz, Th. Schedel-Niedrig, and M. Ch. Lux-Steiner, International Patent No. PCT/DE03/03371.
[11] Th. Glatzel, D. Fuertes Marrón, Th. Schedel-Niedrig, S. Sadewasser, and M. Ch. Lux-Steiner, Appl. Phys. Lett. **81**, 2017 (2002).
[12] D. Fuertes Marrón, Ph.D., thesis Freie Universität Berlin, Germany, 2003.
[13] Ch. Sommerhalter, Th. Matthes, Th. Glatzel, A. Jäger-Waldau, and M. Ch. Lux-Steiner, Appl. Phys. Lett. **75**, 286 (1999).
[14] S. B. Zhang, S.-H. Wei, A. Zunger, and H. Katayama-Yoshida, Phys. Rev. B **57**, 9642 (1998).
[15] Basic differences between Zhang's and Persson's models may however exist linked to the convenience of employing conventional band diagrams for the discussion of GBs.
[16] D. Liao and A. Rockett, J. Appl. Phys. **91**, 1978 (2002).
[17] J. E. Jaffe and A. Zunger, Phys. Rev. B **64**, 241304(R) (2001).
[18] S. B. Zhang and S.-H. Wei, Phys. Rev. B **65**, 081402(R) (2002).
[19] L. Kronik and Y. Shapira, Surf. Sci. Rep. **37**, 1 (1999).
[20] G. Hanna, Th. Glatzel, S. Sadewasser, N. Ott, H. P. Strunk, U. Rau, and J. H. Werner (unpublished).
[21] U. Rau, D. Braunger, R. Herberholz, H. W. Schock, J. F. Guillemoles, L. Kronik, and D. Cahen, J. Appl. Phys. **86**, 497 (1999).